Jackson, E., & Pantony, D. A. (1971) *J. Appl. Electrochem. 1*, 113–126.
Jovanovic, S. V., Harriman, A., & Simic, M. G. (1986) *J. Phys. Chem. 90*, 1935–1939.
Kenney, W. C., & McIntire, W. (1983) *Biochemistry 22*, 3858–3868.
Knappe, J., Neugebauer, F. A., Blaschkowski, H. P., & Gänzler, M. (1984) *Proc. Natl. Acad. Sci. U.S.A. 81*, 1332–1335.
Kober, E. M., Marshall, J. L., Dressick, W. J., Sullivan, B. P., Caspar, J. V., & Meyer, T. J. (1985) *Inorg. Chem. 24*, 2755–2763.
Land, E. J., & Prütz, W. A. (1979) *Int. J. Radiat. Biol. Relat. Stud. 36*, 75–83.
Lytle, F. E., Petrosky, L. M., & Carlson, L. R. (1971) *Anal. Chim. Acta 57*, 239–247.
Mamou, A., Rabani, J., & Behar, D. (1977) *J. Phys. Chem. 81*, 1447–1448.
Margerum, D. W., Chellappa, K. L., Bossu, F. P., & Burce, G. L. (1975) *J. Am. Chem. Soc. 97*, 6894–6896.
Massey, V., & Hemmerich, P. (1980) *Biochem. Soc. Trans. 8*, 246–257.
Mayo, S. L., Ellis, W. R., Crutchley, R. J., & Gray, H. B. (1986) *Science 233*, 948–952.
McLendon, G. (1988) *Acc. Chem. Res. 21*, 160–167.
Meites, L., & Meites, T. (1948) *Anal. Chem. 20*, 984–985.
Melvin, W. S., & Haim, A. (1977) *Inorg. Chem. 16*, 2016–2020.
Merényi, G., Lind, J., & Shen, X. (1988) *J. Phys. Chem. 92*, 134–137.
Miller, J. R. (1987) *Nouv. J. Chim. 11*, 83–89.
Morgan, G., & Burstall, F. H. (1937) *J. Chem. Soc.*, 1649–1655.
Peterson-Kennedy, S. E., McGourty, J. L., Ho, P. S., Sutoris, C. J., Liang, N., Zemel, H., Blough, N. V., Margoliash, E., & Hoffman, B. M. (1985) *Coord. Chem. Rev. 64*, 125–133.
Poulsen, I. A., & Garner, C. S. (1962) *J. Am. Chem. Soc. 84*, 2032–2037.
Prütz, W. A., & Land, E. J. (1979) *Int. J. Radiat. Biol. 36*, 513–520.
Prütz, W. A., Butler, J., Land, E. J., & Swallow, A. J. (1980) *Biochem. Biophys. Res. Commun. 96*, 408–414.
Prütz, W. A., Land, E. J., & Sloper, R. W. (1981) *J. Chem. Soc., Faraday Trans. 1 77*, 281–292.
Ram, M. S., & Stanbury, D. M. (1986) *J. Phys. Chem. 90*, 3691–3696.
Reichard, P., & Ehrenberg, A. (1983) *Science 221*, 514–519.
Schilt, A. A. (1969) in *Analytical Applications of 1,10-Phenanthroline and Related Compounds* (Belcher, R., & Freiser, H., Eds.) Vol. 32, International Series of Monographs in Analytical Chemistry, Pergamon Press, Oxford, U.K.
Szentrimay, R., Yeh, P., & Kuwana, T. (1977) in *Electrochemical Studies of Biological Systems* (Sawyer, D. T., Ed.) ACS Symposium Series 38, pp 143–169, American Chemical Society, Washington, DC.
Troitskaya, N. V., Mishchenko, K. P., & Flis, I. E. (1959) *Russ. J. Phys. Chem. 33*, 77–79.
Wilmarth, W. K., Stanbury, D. M., Byrd, J. E., Po, H. N., & Chua, C. P. (1983) *Coord. Chem. Rev. 51*, 155–179.

Solution Conformation of Conotoxin GI Determined by ^{1}H Nuclear Magnetic Resonance Spectroscopy and Distance Geometry Calculations

Yuji Kobayashi,*,‡ Tadayasu Ohkubo,‡,§ Yoshimasa Kyogoku,‡ Yuji Nishiuchi,∥ Shumpei Sakakibara,∥ Werner Braun,⊥,○ and Nobuhiro Gō○,△

Institute for Protein Research, Osaka University, Suita, Osaka 565, Japan, Peptide Institute Inc., Protein Research Foundation, Ina, Minoh, Osaka 562, Japan, and Department of Physics, Faculty of Science, Kyushu University, Kyushu 812, Japan

Received November 30, 1988; Revised Manuscript Received February 8, 1989

ABSTRACT: Conformational analysis of conotoxin GI, one of the neurotoxic peptides produced by a marine snail, genus *Conus*, was performed by a combination of nuclear magnetic resonance spectroscopy (NMR) and distance geometry calculations. The resulting conformers on minimization of the target function were classified into two groups. The difference in the structures of the conformers is mainly due to the difference in the orientation of the side chain of the tyrosyl residue. The results show that the solution structure of conotoxin GI satisfies the conformational requirements for the biological activity of an antagonist toward nicotinic cholinergic receptors elucidated in a series of studies on alkaloids. The structure is discussed on the basis of the results of comparison of the atomic arrangements of the active sites of snake venom peptides and molecular models based on the results of secondary structure prediction.

Fish-eating marine snails of the genus *Conus* produce several classes of toxic peptides that specifically bind to key elements in nerve and muscle cell membranes, resulting in successive blocking of the series of neuromuscular systems of fish (Kohn et al., 1960; Endean & Rudkin, 1963; Spence et al., 1977; Cruz et al., 1978; Olivera et al., 1985). They are called conotoxins and are classified into three large groups: α-conotoxins are presynaptic (Gray et al., 1984; McIntosh et al., 1982), ω-conotoxins are postsynaptic (Olivera et al., 1984, 1987), and μ-conotoxins are muscle channel inhibitors (Cruz et al., 1985). Gray et al. have systematically studied these peptides and have shown that commonly they are relatively small peptides of 13–29 amino acid residues and include 2–3 disulfide bonds.

* Author to whom correspondence should be addressed.
‡ Osaka University.
∥ Present address: Protein Engineering Research Institute, Suita, Osaka 565, Japan.
∥ Peptide Institute Inc.
⊥ Present address: Institute fur Molekularbiologie u. Biophysik, ETH, CH-8093 Zurich, Switzerland.
○ Kyushu University.
△ Present address: Department of Physics, Faculty of Science, Kyoto University, Kyoto 606, Japan.

0006-2960/89/0428-4853$01.50/0

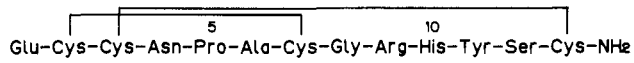

FIGURE 1: Amino acid sequence of conotoxin GI from *C. geographus* (Gray et al., 1981; Nishiuchi & Sakakibara, 1982).

As α-conotoxins, three related peptide toxins consisting of 13–15 amino acid residues were isolated from the venom of *Conus geographus* and shown to block synaptic transmission by binding to the acetylcholine receptor, thus causing paralysis (Gray et al., 1981; McIntosh et al., 1982). These three peptides, designated conotoxins GI, GIa, and GII, were chemically synthesized, and the modes of their disulfide formations were revealed (Nishiuchi & Sakakibara, 1982; Gray et al., 1984).

The molecular conformation of conotoxin GI was deduced by means of model building through secondary structure analysis involving circular dichroism (CD)[1] measurements and Chou and Fasman's method of prediction (Hider, 1985; Gray et al., 1985; Chou & Fasman, 1974). Its toxic activity is similar to those of snake α-neurotoxins of 60–70 amino acid residues (Yang, 1974; McManus et al., 1981). These toxins have been well investigated in relation to curare-like alkaloids, which show potent ability to block the nicotinic acetylcholine receptor (Pauling & Petcher, 1973; Hider & Dufton, 1979). Comparison of their structures has suggested that there is a strong resemblance between the conformation of conotoxin GI and those of the reactive centers, so-called active tips, of snake α-neurotoxins (Dufton & Hider, 1977, 1980, 1983; Low et al., 1976; Tsernoglou & Petsko, 1976).

To test the structure of the model, we have determined the three-dimensional structure of conotoxin GI in solution. The structure was elucidated through the combined use of ^{1}H NMR and a distance geometry algorithm (Braun et al., 1981; Braun & Gō, 1985; Ohkubo et al., 1986). The results obtained for this small peptide with such remarkable activity should provide a good explanation for the structure–activity relationship of conotoxin GI.

Materials and Methods

Sample. Conotoxin GI, the amino acid sequence of which is shown in Figure 1, was synthesized and its activity demonstrated as described previously (Gray et al., 1981; Nishiuchi & Sakakibara, 1982). The chemical synthesis provided a sufficient amount for NMR measurements, especially for two-dimensional NMR. Deuterated dimethyl sulfoxide (DMSO-d_6) was used as the solvent, and the concentration of the solution was 8 mM.

NMR Spectroscopy. Proton NMR spectra were recorded at 500 MHz on a JEOL GX-500 spectrometer. Two-dimensional spectra on nuclear Overhauser effect spectroscopy (NOESY) (Kumar et al., 1980), double quantum filtered chemical shift correlated spectroscopy (DQF-COSY) (Rance et al., 1983), and homonuclear Hartmann–Hahn spectroscopy (HOHAHA) (Davis & Bax, 1985) were recorded in the phase-sensitive detection mode by the four-quadrant method proposed by States et al. (1982). The NOESY spectra were recorded with various mixing times, 100, 120, and 200 ms, for evaluation of the effects of spin diffusion and coherent magnetization transfer. The HOHAHA spectra were also recorded with various mixing times, 25.1, 43.0, 65.5, and 95.5 ms, to follow successively direct, single, and multiple relayed through-bond connectivities. The sizes of the data in time domains were 2K points for the t_2 direction and 256 points for the t_1 direction. The digital resolutions in the cases of NOESY and HOHAHA spectra were 10.74 Hz/point in the ω_1 direction and 5.37 Hz/point in the ω_2 direction. These were obtained by zero filling in the ω_1 direction. All NMR measurements were carried out at 20 °C.

Calculations. To calculate the conformation that satisfied the distance constraints between paired protons in the molecule, minimization of the variable-target function was carried out with the DADAS program as described by Braun and Gō (1985) and Ohkubo et al. (1986). The ACOS 2000 mainframe computer at the computer center of Osaka University was used. Analysis of the structures and molecular drawings were carried out with the VENUS program for the ACOS 900 computer at the Crystallographic Research Center, Institute for Protein Research, Osaka University (Iga & Yasuoka, 1984).

Results and Discussion

Assignment of the ^{1}H NMR Spectrum. The sequence-specific resonance assignment procedure introduced by Wüthrich et al. was used to make whole peak assignments as follows (Wuthrich, 1986).

First, amino acid spin systems were identified by surveying direct and relayed through-bond connectivities in the DQF-COSY and HOHAHA spectra. Figure 2 shows the NH aliphatic region of the HOHAHA spectrum. The HOHAHA spectra series were generally more useful for delineating the spin-coupling connectivities than the DQF-COSY spectra. Thus, the latter were used rather complementarily.

The protons of the aromatic rings of His^{10} and Tyr^{11} were identified on the basis of the through-space connectivities to individual C_β protons in the NOESY spectra. The amide protons of the side chain of Asn^4 and the C-terminus of the peptide were also connected to the corresponding C_β protons of Asn^4 and Cys^{13}, respectively, in the NOESY spectra. The OH proton of Ser^{12} and the ζ-NH_2 protons of Arg^9 were missing in all spectra. These signals might be broadened due to the fast exchange of such labile protons with those of water, which was present in the DMSO-d_6 in an extremely small amount. The backbone NH's of Arg^9 and Tyr^{11} were detected only in the case of the sequential nuclear Overhauser effect (NOE) connectivities with the corresponding C_α protons of Gly^8 and His^{10}, respectively. The individual protons belonging to Glu^1, Pro^5, Ala^6, Gly^8, Arg^9, and Ser^{12} were easily assigned on the basis of their coupling profiles; the spin systems of these six residues are unique, respectively, in the molecule, so their coupling patterns are distinguishable from the others.

Next, assignment of the resonances of the remaining residues including four cysteinyl residues was carried out by means of sequential assignment using NH–C_αH, NH–NH, and NH–C_βH proton connectivities. Figure 3 shows the NOESY–COSY connectivity diagrams, where the assignment pathway is alternately demonstrated by indicating COSY connectivities, NH(i)–C_αH(i), and NOESY connectivities, C_αH(i)–NH(i + 1). Although the network is interrupted at Asn^4 because of a lack of NH in Pro^5, there is a through-space connectivity between the C_α proton of the former and the C_δ protons of the latter. Table I lists the resonance assignments.

Some satellite signals were detected in the spectra, as indicated in Figures 4 and 5. Figure 4, which is a part of the HOHAHA spectrum, shows that Pro^5 and Ala^6 exist in two

[1] Abbreviations: NMR, nuclear magnetic resonance; CD, circular dichroism; DMSO-d_6, deuterated dimethyl sulfoxide; NOESY, nuclear Overhauser effect spectroscopy; DQF-COSY, double quantum filtered chemical shift correlated spectroscopy; HOHAHA, homonuclear Hartmann–Hahn spectroscopy; DADAS, distance analysis in dihedral angle space; NOE, nuclear Overhauser effect; HPLC, high-performance liquid chromatography; rmsd, root mean square distances.

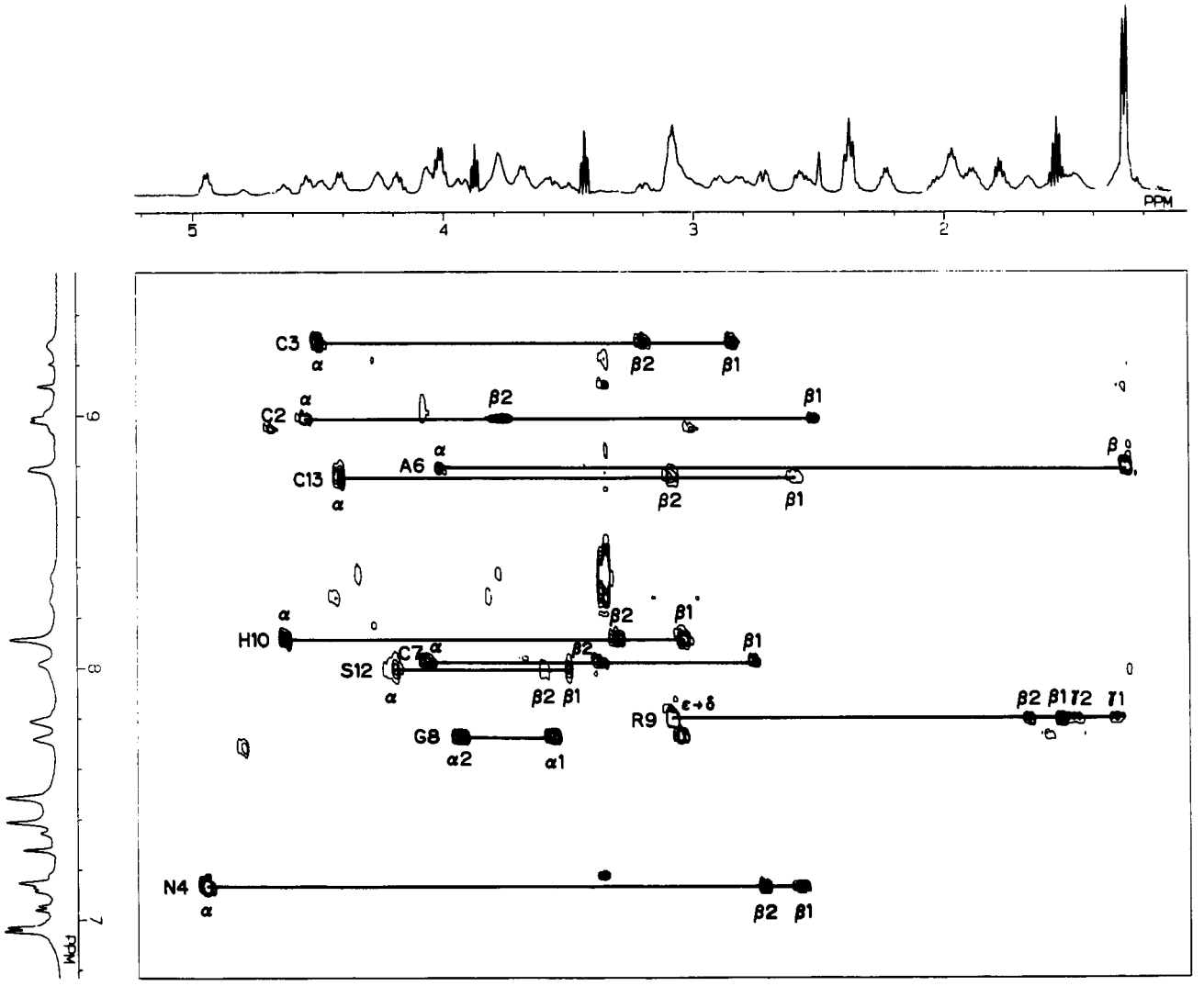

FIGURE 2: NH aliphatic region of the HOHAHA spectrum of conotoxin GI in DMSO-d_6. Horizontal lines show the intraresidual spin-coupling connectivities. The backbone NH's of Glu[1], Arg[9], and Tyr[11] are missing. The connectivity for Arg[9] is demonstrated with $N_\epsilon H$–$C_\delta H$.

states. Each minor peak was assigned, respectively, on the basis of its unique spin system. The differences in chemical shifts of each satellite peak from those of the corresponding major peaks are so small, except for those of C_α protons, that the existence of an isomer was only detectable in the two-dimensional spectra. No NOE connectivities were detected between major and minor peaks in NOESY spectra, even with the long mixing time, 200 ms. Thus, the conformational exchange between these isomers should be slow. Although no satellite signal at Asn[4] was detectable, such an interconversion is generally attributable to the cis–trans isomerization at the X–Pro peptide bond (Torchia, 1972; Cheng & Bovey, 1977).

Other satellite signals were found at Tyr[11]. As shown in Figure 5, the signals of aromatic and OH protons carried satellite signals besides the major peaks. The isomerization around the Tyr[11] residue is not clear so far. This could not be attributed to the prolyl cis–trans isomerization because the ratios of the peak intensities are quite different from those in the cases of Pro[5] and Ala[6]. Such an isomerization around the Tyr residue was also found in the NMR spectra of conotoxin MI, which is a homologue of conotoxin GI produced by *Conus magus*. The ^1H NMR spectrum of conotoxin MI showed such satellites of which the intensities depend largely on the solvent and temperature, and no NOE connectivities were detected among major and minor peaks of Tyr[12] residue of conotoxin MI (Kobayashi et al., unpublished data). These phenomena, which should be due to some isomerization, had been detected in the HPLC profiles of conotoxin MI as well (Gray et al., 1983; Nishiuchi & Sakakibara, 1984). The details of the isomerization of conotoxin GI, in relation to conotoxin MI, are under investigation.

Other paired peaks at 7.18 and 7.35 ppm were observed, as can be seen in Figure 5. However, assignment of these peaks was not possible because there were no connectivities detected with these peaks, i.e., as if they are isolated from all the others.

Judging from these findings, there appear two types of conformational isomerism in conotoxin GI in DMSO. However, the rates of the interconversions were so slow that no correlation peak between the isomers was detected in the NOESY spectra, and the intensities of the satellite peaks were quite weak. Furthermore, the conformational isomerizations are localized. Thus, both of these isomerizations were neglected in the overall structure determination.

Secondary Structure. Because conotoxin GI is so small and is constrained by two disulfide bonds, a common secondary structure cannot be much expected. However, Hider found on curve fitting of the CD spectrum of conotoxin GI that the spectrum shows a high α-helical content of up to 50%. He carried out secondary structure prediction by means of the modified Chou and Fasman method and postulated a structure with an α-helical region between Cys[6] and His[10], without interruption by two disulfide bonds and the Pro[5] residue (Hider, 1985).

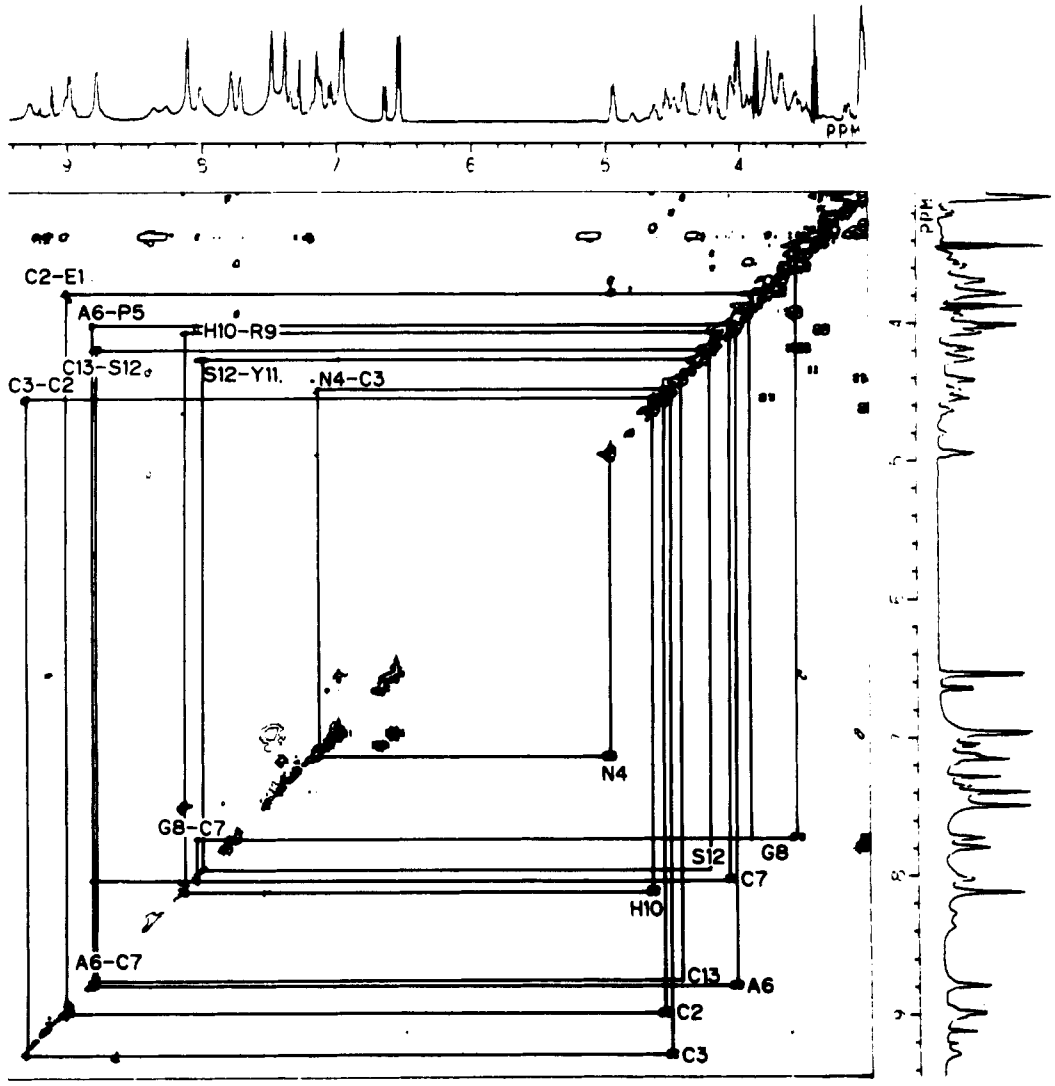

FIGURE 3: NOESY–COSY connectivity diagram for sequential assignments. The lower right triangle was taken from the COSY spectrum of conotoxin GI in DMSO-d_6 solution. The cross peaks corresponding to intraresidual spin couplings between $C_\alpha H$ and NH are labeled. Such cross peaks of E1, P5, R9, and Y11 are missing. The upper left triangle was taken from the NOESY spectrum of the same sample with a mixing time of 120 ms. The cross peaks corresponding to NOE connectivities between $C_\alpha H_i$ and NH(i + 1) are labeled. The assignment pathway is demonstrated by indicating alternative COSY and NOESY connectivities. These are interrupted at N4–P5, G8–R9, and H10–Y11 because of the lack of NH's. The NOE connectivites between NH(i) and NH(i + 1) were used for the junctions at A6–C7 and C7–G8.

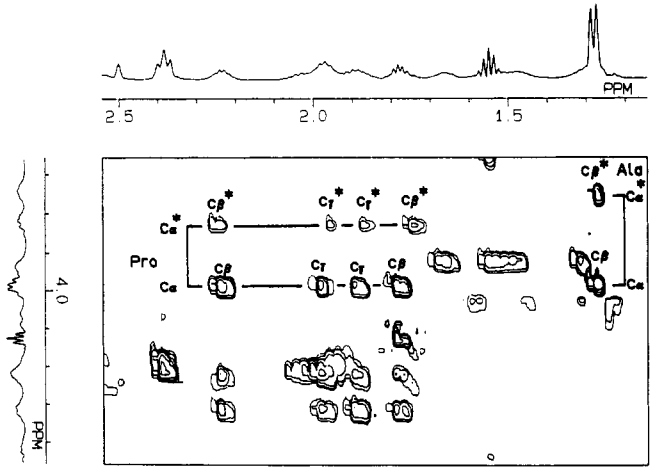

FIGURE 4: Part of the aliphatic region (ω_2 1.25–2.55 ppm, ω_1 3.65–4.45 ppm) of the HOHAHA spectrum of conotoxin GI in DMSO-d_6. Horizontal lines at 1.7–2.4 ppm connect the two spin-coupling networks of the pyrrolidine ring corresponding to the major and minor peaks of $C_\alpha H$ of Pro[5]. The peaks of the minor component are indicated by an asterisk. The peaks around 1.3 ppm are $C_\beta H$ of Ala[6] connected to the major and minor peaks of C_α of Ala[6], respectively.

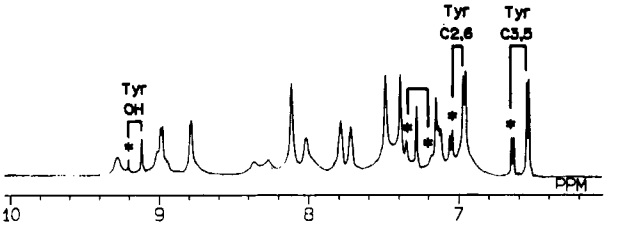

FIGURE 5: Part of the one-dimensional spectrum of conotoxin GI in DMSO-d_6. The signals of aromatic CH and OH protons of Tyr[11] are shown with their satellite signals indicated by an asterisk. The paired signals at 7.18 and 7.35 ppm could not be assigned.

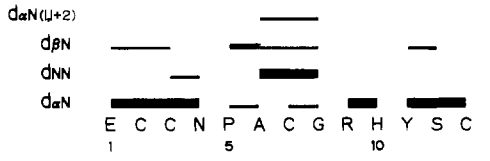

FIGURE 6: Sequential and medium-range NOEs detected in the NOESY spectrum of conotoxin GI. $d_{\alpha N}$ represents NOE between $C_\alpha H(i)$ and NH(i + 1), where i is the residual number. d_{NN} represents NOE between NH(i) and NH(i + 1). $d_{\beta N}$ represents NOE between $C_\beta H(i)$ and NH(i + 1). The thickness of the lines indicates the relative intensities of cross peaks in the NOESY spectrum.

Table I: Resonance Assignments for Conotoxin GI in DMSO-d_6 at 20 °C[a]

	NH	$C_\alpha H$	$C_\beta H$	$C_\gamma H$	$C_\delta H$	$C_\epsilon H$	OH
Glu[1]	8.27	3.78	1.96	2.38			
	8.36		2.01				
Cys[2]	8.95	4.54	2.52				
			3.77				
Cys[3]	9.28	4.49	2.82				
			3.19				
Asn[4]	7.13	4.94	2.56		7.49		
			2.71		8.11		
Pro[5]		4.00	1.78	1.88	3.68		
			2.23	1.97	3.77		
Ala[6]	8.79	4.01	1.28				
Cys[7]	8.02	4.05	2.75				
			3.36				
Gly[8]	7.71	3.54					
		3.92					
Arg[9]		4.07	1.52	1.31	3.08	7.79	
			1.66	1.46			
His[10]	8.10	4.62	3.03		7.26	8.95	
			3.30				
Tyr[11]		4.25	2.79		6.96	6.54	9.12
					(7.05)	(6.64)	(9.21)
			2.89				
Ser[12]		4.18	3.61				
			3.50				
Cys[13]	8.74	4.41	2.56		7.15		
			3.07		7.39		

[a] All chemical shift values are given in parts per million from tetramethylsilane. The numbers in parentheses are the chemical shifts of satellite signals.

The regular secondary structure elements of polypeptides can be elucidated by analyzing the sequential and medium-range NOEs (Wüthrich et al., 1984). By investigating these NOEs, as found in the NOESY spectra of conotoxin GI and summarized in Figure 6, the secondary structure of conotoxin GI in solution was examined to test this postulated chain folding. In the NOESY spectra, strong NOEs between $C_\alpha H(i)$ and $NH(i + 1)$, $d_{\alpha N}$, were detected at residues i = 1–3, 9, 11, and 12. These NOEs are indicative that these segments of polypeptides are almost fully extended or in β-sheet structures. Weak $d_{\alpha N}$ NOEs were detected at residues i = 5 and 7 as well. Strong NOEs between $NH(i)$ and $NH(i + 1)$, d_{NN}, were found at residues i = 6 and 7 and weak NOEs at residue i = 3. The d_{NN} NOEs indicate the local arrangements of conformation in an α-helix or a type I β-turn structure. A weak NOE between $C_\alpha H(i)$ and $NH(i + 2)$ was detected at residues i = 6. These profiles of sequential and medium-range NOE connectivities in the range 5–8 suggest that a turn I structure should exist in this region. This region corresponds to the segment for which the secondary structure was predicted to be in an α-helical conformation by Hider (1985).

The other combination of weak $d_{\alpha N}$ and d_{NN} suggests another type I β-structure in the sequence around 3–4 as well. The existence of β-turn structures was predicted by Gray et al. in the regions Asn[4]–Cys[7] and Gly[8]–Tyr[11] by means of Chou and Fasman's method (Gray et al., 1985; Chou & Fasman 1974; Wemmer & Kallenbach, 1983).

At this stage, it could be said that the places where ordered structures, α-helix or β-turn, had been predicted correspond roughly to the two regions where turn I structures were found through the NOE connectivities.

Distance Constraints. The interresidual NOE connectivities, which were detected in the NOESY spectra and used for the calculation, are presented in a diagonal plot in Figure 7.

The intensities of the NOE peaks were translated into the corresponding atomic distances in the following way (Braun et al., 1981).

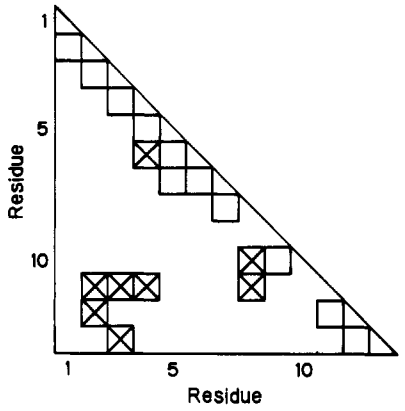

FIGURE 7: Diagonal plot of the NOE connectivities used as distance constraints in the conformation determination of conotoxin GI in DMSO-d_6. Both axes represent the amino acid sequence. Open squares indicate that NOEs between backbone protons of two residues corresponding to each sequential location were observed. Squares with crosses indicate NOEs between a proton of a residue and a side-chain proton of another residue. An interresidual side chain–side chain NOE was not detected.

The observed NOEs were classified into two groups, i.e., short-range NOEs, which are intraresidual NOEs and those between backbone hydrogen atoms and C_β protons of adjacent residues, and long-range NOEs, which are those between the remaining pairs of protons. The intensities of short-range NOEs were interpreted by means of a rigid model. In this model, the fluctuation of the distance was assumed to be so small that the intensity of an NOE should be related to the atomic distance according to the equation of the general form, $NOE \propto 1/r^6$.

The short-range NOEs were classified as weak, medium, or strong, by counting the contour lines in contour plots of the NOESY spectra, and the corresponding upper distance constraints were calibrated relative to the standard distance to be 3.5, 3.0, and 2.5 Å, respectively (Williamson et al., 1985). The standard for calibrating relative intensities was provided by the intensity of the NOE between two C_β protons of a Cys residue that showed the strongest NOE intensity among all pairs of C_β protons. The distances between these protons were estimated to be 1.75 Å. The upper distance constraints between the paired atoms that showed long-range NOEs were assumed to be 4 Å, adopting the idea of the threshold value of distance where an NOE was first detected. Such treatment of long-range NOEs was discussed previously (Ohkubo et al., 1986).

The lower distance constraints were assumed throughout to be the sum of the core radii of the two protons, i.e., 2.0 Å. Additional distance constraints were provided by the two disulfide bonds. When some NOE peaks for side-chain protons could not be assigned stereospecifically, interpretation of these NOEs was carried out by using so-called pseudoatoms as reference points for distance constraints following the method suggested by Wüthrich (1986).

Distance Geometry Calculation. To elucidate the three-dimensional structure of conotoxin GI in solution on the basis of experimental interproton distances determined by NOE measurement, Braun and Gō's method was used (Braun & Gō, 1985). It consists of minimization of the square sum of the differences between atomic distances in the calculated structure and the corresponding distances obtained from NOE information. The details of the procedure were given in a previous paper with an example of application to a toxic peptide, STh (Ohkubo et al., 1986).

Table II: Root Mean Square Distances (rmsd) among 10 Conformers with the Lowest 10 Residual Values for the Target Function[a]

I	0.24	*	2.46	2.21	2.73	4.69	4.91	4.80	4.86	4.74	4.57
IV	0.39	1.77	*	1.67	3.30	4.30	4.55	4.04	4.09	4.25	3.82
V	0.47	1.48	1.05	*	2.93	4.15	4.41	3.90	4.14	3.99	3.73
IX	0.57	1.77	2.13	1.67	*	3.90	3.70	4.80	4.35	4.67	4.40
II	0.29	3.90	3.16	3.18	2.78	*	1.74	2.98	2.61	3.22	2.93
III	0.29	3.62	2.92	2.94	2.36	1.06	*	3.26	2.30	3.38	3.36
VI	0.50	3.56	2.61	2.66	2.93	1.62	1.70	*	2.34	2.13	1.63
VII	0.56	3.69	2.61	2.82	2.91	1.64	1.46	1.13	*	3.13	2.42
VIII	0.56	3.63	2.97	2.94	2.91	1.89	1.65	1.43	1.73	*	2.34
X	0.59	3.53	2.60	2.60	2.88	1.67	1.77	0.35	1.21	1.43	*
		I	IV	V	IX	II	III	VI	VII	VIII	X

[a]The first column shows the residual values for the target function. The lower left triangle shows the rmsd calculated for the backbone atoms and the upper right triangle that for all atoms.

First, the error function, T, for a given set of constraints is determined as the target function to be minimized

$$T = \sum' \frac{(U_{ij}^2 - r_{ij}^2)^2}{U_{ij}^2} + \sum' \frac{(L_{ij}^2 - r_{ij}^2)^2}{L_{ij}^2} + \sum' w[(s_i + s_j)^2 - r_{ij}^2]^2 \quad (1)$$

where r_{ij}, U_{ij}, and L_{ij} are the interatomic distance between atoms i and j, and the upper and lower constraints of the corresponding r_{ij}, respectively. s_i and s_j are the repulsive core radii of the i and j atoms. $\sum'$ means summation only over the terms that violate distance constraints, and w is the weight of the third term relative to that of the first and second terms.

Next, an initial conformation is generated by using random values for dihedral angles, and r_{ij} are calculated. Then the target function is minimized by changing the values for the dihedral angles, with fixed values for bond angles and bond lengths of peptide residues. To avoid the multiple minimum problem during the minimization, the distance constraints are applied stepwise according to the difference between residue numbers to which each of the paired protons under consideration belongs. Starting from the conformation obtained in the previous stage, a series of minimizations is then carried out with constraints between further residues along the primary structure.

These calculations were carried out with the DADAS computer program written by Braun and Gō (1985).

Results of the Calculations. Starting from 100 initial conformations, which were chosen individually and randomly, an assembly of 100 conformers was obtained by repetition of the calculations. Although the value for the target function, T, should vanish if the resulting conformation satisfies all the constraints, each resulting conformer actually retains some value for the target function at the final stage of each series of minimizations. These values indicate the extent to which each conformer satisfies the constraints. The resulting conformers were numbered I, II, III, ... according to the residual value of the target function, from the smallest value. Ten conformers, I–X, that best satisfy the constraints were picked and compared to judge how these structures converge on each other. The convergence was examined in terms of the root mean square distances (rmsd) among each of the 10 conformers.

Analysis of these rmsd values revealed the following interesting relationships among the conformers. As shown in Table II, they can be classified into two groups, A and B. Group A consists of conformers I, IV, V, and IX and group B of conformers II, III, VI–VIII, and X. Although the average value for rmsd calculated for backbone atoms among all 10 conformers is 2.32 Å, that among the conformers of group A is 1.58 Å and that for group B 1.45 Å. The values calculated for all atoms are 3.54, 2.52, and 2.61 Å, respectively. This shows that the minimization leads to two kinds of conformations. The major difference in conformation between the two groups appears to be the different orientation of the side chain of Tyr^{11}.

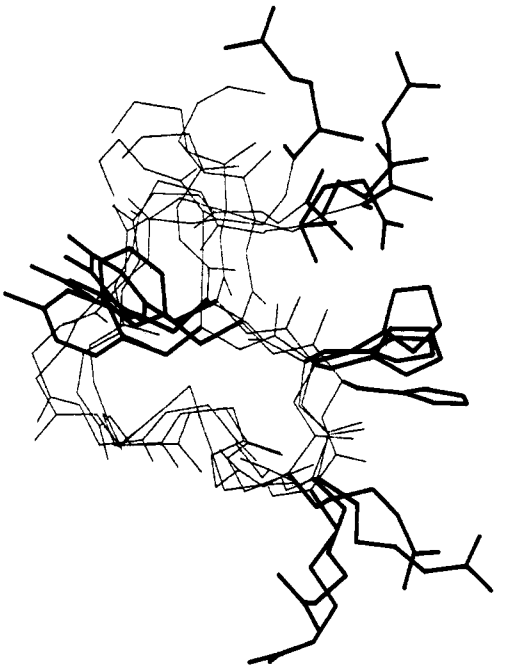

FIGURE 8: Backbone conformations of the four conformers, I, IV, V, and IX of group A, of conotoxin GI calculated with the DADAS program, plotting only backbone atoms N, C_α, C′. The side chains of Glu^1, Arg^9, His^{10}, and Tyr^{11} are drawn as bold lines. The structures were superimposed so as to get the best fit in the space.

Why the minimization led to the convergence into two conformers is not clear at present. The main reason should be the lack of NOE connectivities around the Tyr^{11} residue. Investigation of the dynamics of this molecule is in progress. At this stage both conformers should be candidates for the conformation of conotoxin GI.

The resulting conformers of each group are illustrated, respectively, in Figures 8 and 9, drawing the bonds connecting the backbone atoms, N, C_α and C′ atoms, and superimposed to get the best fit in the space.

Conformation of Conotoxin GI in Solution. The aim of this structural study was to obtain information on the structure–activity relationships of conotoxin GI. Although there has been discussion of the structural resemblance between conotoxin GI and other toxins in the literature, it was based on hypothetical structures for conotoxin GI derived by means of the Chou and Fasman method of prediction. Using the structure presented in Figures 8 and 9, even with the limitation that

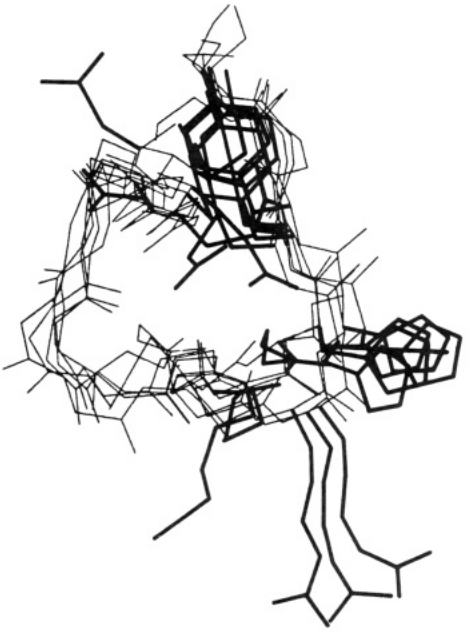

FIGURE 9: Backbone conformations of the six conformers, II, III, VI–VIII, and X of group B, of conotoxin GI calculated with the DADAS program, plotted in the same way as in Figure 8.

DMSO was used as the solvent, we can now provide additional support to these hypothetical structures and cultivate a better understanding of the structure–activity relationships.

A series of alkaloids, which block the neurotransmission at the neuromuscular junction, for example, *d*-tubocurarine and *C*-alkaloid E, have been investigated extensively by X-ray analysis. The structural requirements of such antagonists toward nicotinic cholinergic receptors for physiological activity were elucidated by Pauling and Petcher (1973) to be as follows: (i) a rigid conformation; (ii) two quaternary nitrogen atoms separated by 10.8 ± 0.3 Å; (iii) a sufficient degree of lipophilicity in the gap between the two cationic centers; and (iv) oxygen atoms disposed to aid the molecular orientation.

Dufton and Hider demonstrated that these requirements could be satisfied in the case of neurotoxic polypeptides of snake venoms. They pointed out that the active tip of erabutoxin *b*, a snake venom, could have a disposition of amino acid side chains satisfying these requirements, such that Arg^{33} and Lys^{47} act as the cationic centers and Phe^{32} and Tyr^{29} provide the lipophilicity (Dufton & Hider 1977; Hider & Dufton, 1979). Such a disposition itself was not found in the structure determined on X-ray analysis of a crystal of erabutoxin *b* (Kimball et al., 1979). They postulated the existence of some flip-flop movements around the active tip in solution that modify the structure, so as to resemble those of the alkaloids. Such modifications of the structure, requiring conformational equilibrium in solution, were supported by the observance of flexibility in the conformations of the neurotoxic peptide as detected in the reported NMR and CD studies (Hider & Dufton, 1979; Dufton & Hider 1980, 1983).

When taking into consideration such factors as invariant residues and the predicted secondary structure of α-conotoxin and the resemblance of the neurotoxic activities of conotoxin GI to those of snake venoms, it was postulated that the N-terminus of Glu^1 acts as one of the cationic centers, the side chain of Arg^9 acts as another cationic center, and His^{10} and Tyr^{11} are located between these two centers (Hider, 1985).

The spatial arrangements of these four amino acid residues of conotoxin GI in the calculated structures are shown in Figures 8 and 9. It is obvious that the arrangements of these residues in the group A structures in Figure 8 fit the postulated

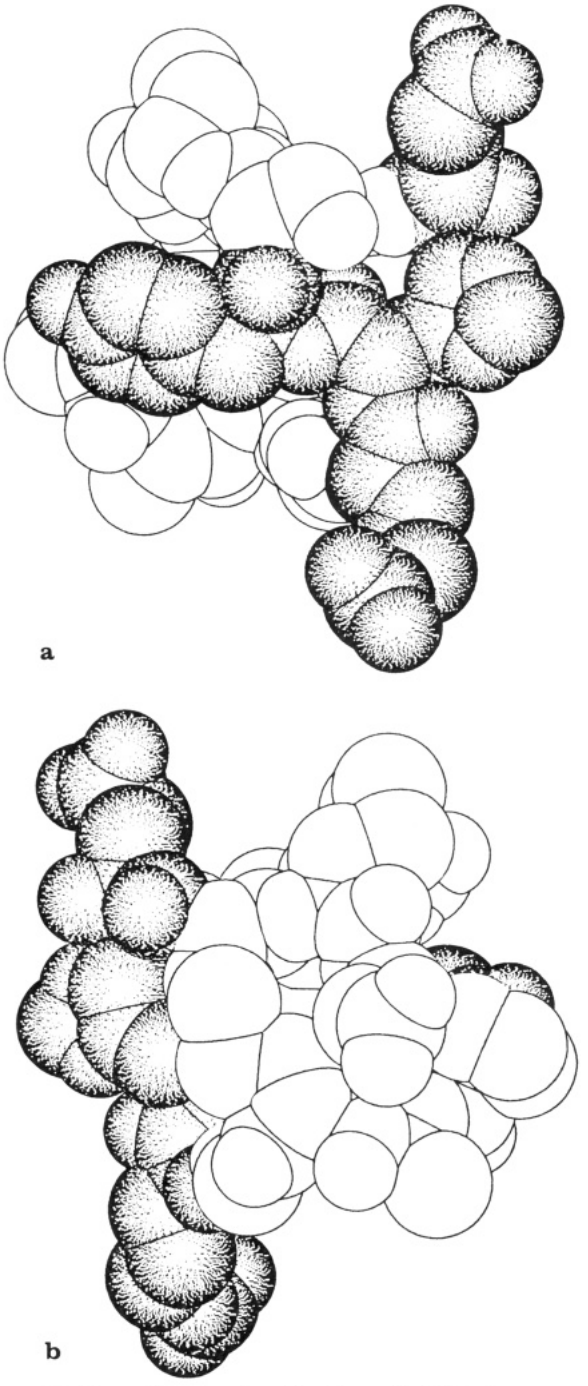

FIGURE 10: Space-filling drawing of conformer I with the lowest target function value with the DADAS program as a representative structure of conotoxin GI in solution. The four residues related to the conformational requirement for biological activity, Glu^1, Arg^9, His^{10}, and Tyr^{11}, are shadowed. (a) is the front view of the molecule where these four residues were localized, and (b) is the reverse view.

model surprisingly well. In Figure 10, a space-filling drawing of conformer I is presented as a representative group A conformation.

The group B structures in Figure 9 show better agreement with the model of conotoxin GI deduced by Gray et al., according to the results of secondary structure prediction, which shows a strong resemblance to that of the active tip of erabutoxin *b* (Gray et al., 1985). Although the backbone structures look quite similar to each other, there are, of course, disagreements in detail that may be due to overestimations during the prediction. The salt bridge between the side chains of Glu^1 and Arg^9, postulated in the model, was not found in

the calculated structures, so there should be a rather low probability of its formation. One explanation for this is that the solvent used in this structure determination was DMSO, while the prediction was carried out with the expectation of an aqueous solution. In fact, a pH titration experiment on an aqueous solution of conotoxin GI did not give any indication of such a salt bridge (Kobayashi et al., unpublished data). Although the presence of a regularly tight turn conformation in the calculated structure is not as clear, the mode of the chain fold of the backbone looks essentially consistent with that of the model determined by Gray et al., i.e., the formation of two β-turns starting at Asn^4 and Gly^8. The profile of NOE connectivities in the NMR spectrum of conotoxin GI and the dihedral angles of the backbone chains of the calculated structure indicate that some highly constrained structures exist around the segments where β-turns were postulated. Such a profile also suggests that the possibility of the presence of an α-helical conformation in the region between Ala^6 and His^{10}, which was predicted by Hider to explain the CD spectrum of conotoxin GI indicating a high α-helical content of up to 50%, should be low. The CD pattern could reflect some partial arrangements of dipole moments of peptides in the constrained segment.

While some ambiguities remain in the detailed structure because of the rather poor convergence, we have thus demonstrated that conotoxin GI takes on a spatial atomic arrangement in solution with features similar to those of a series of alkaloids, which are antagonists toward nicotinic cholinergic receptors. These similarities are of the same sort as those postulated by Dufton and Hider in the case of neurotoxin peptides of snake venoms (1980).

To obtain further information on the structure–activity relationships of neurotoxins, we are currently determining the structures of chemical derivatives of conotoxins GI and MI, for which the biological activities have been investigated, in comparison with those of native conotoxins. The results should provide some information on nicotinic receptors as well.

Registry No. Conotoxin GI, 76862-65-2.

References

Braun, W., & Gō, N. (1985) *J. Mol. Biol. 186*, 611–626.

Braun, W., Bosch, C., Brown, L. R., Gō, N., & Wüthrich, K. (1981) *Biochim. Biophys. Acta 667*, 337–396.

Cheng, H. N., & Bovey, F. A. (1977) *Biopolymers 16*, 1465–1472.

Chou, P. Y., & Fasman, G. D. (1974) *Biochemistry 13*, 211–222.

Cruz, L. J., Gray, W. R., & Olivera, B. M. (1978) *Arch. Biochem. Biophys. 190*, 539–548.

Cruz, L. J., Gray, W. R., Olivera, B. M., Zeikus, R. Z., Kerr, L., Yoshikami, D., & Moczydlowski, E. (1985) *J. Biol. Chem. 260*, 9280–9288.

Davis, D. G., & Bax, A (1985) *J. Am. Chem. Soc. 107*, 2820–2821.

Dufton, M. J., & Hider, R. C. (1977) *J. Mol. Biol. 115*, 177–193.

Dufton, M. J., & Hider, R. C. (1980) *Trends Biochem. Sci. 5*, 53–56.

Dufton, M. J., & Hider, R. C. (1983) *CRC Crit. Rev. Biochem. 14*, 113–171.

Endean, R., & Rudkin, C. (1963) *Toxicon 1*, 46–64.

Gray, W. R., Luque, A., Olivera, B. M., Barrett, J., & Cruz, L. J. (1981) *J. Biol. Chem. 256*, 4734–4740.

Gray, W. R., Rivier, J. E., Galyean, R., Cruz, L. J., & Olivera, B. M. (1983) *J. Biol. Chem. 258*, 12247–12251.

Gray, W. R., Luque, F. A., Galyean, R., Atherton, E., Sheppard, R. C., Stone, A., Reyes, A., Alford, J., McIntosh, M., Olivera, B. M., Cruz, L. J., & Rivier, J. (1984) *Biochemistry 23*, 2796–2802.

Gray, W. R., Middlemas, D. M., Zeikus, R., Olivera, B. M., & Cruz, L. J. (1985) in *Peptides: Structure and Function* (Deber, C. M., Hruby, V. J., & Kopple, K. D., Eds.) pp 823–832, Pierce Chemical Co., Rockford, IL.

Hider, R. C. (1985) *FEBS Lett. 184*, 181–184.

Hider, R. C., & Dufton, M. J. (1979) in *Natural Toxins* (Eakere, D., & Wadstrom, T., Eds.) pp 515–522, Pergamon, London.

Iga, Y., & Yasuoka, N. (1984) *J. Mol. Graphics 2*, 79–82.

Kimball, M. R., Sato, A., Richardson, J. S., Rosen, L. S., & Low, B. W. (1979) *Biochem. Biophys. Res. Commun. 88*, 950–959.

Kohn, A. J., Sanders, P. R., & Wiener, S. (1960) *Ann. N.Y. Acad. Sci. 90*, 706–725.

Kumar, A., Ernst, R. R., & Wüthrich, K. (1980) *Biochem. Biophys. Res. Commun. 95*, 1–6.

Low, B. W., Preston, H. S., Sato, A., Rosen, L. S., Searle, J. E., Rudko, A. D., & Richardson, J. S. (1976) *Proc. Natl. Acad. Sci. U.S.A. 73*, 2991–2994.

McIntosh, M., Cruz, L. Z., Hunkapiller, M. W., Gray, W. R., & Olivera, B. M. (1982) *Arch. Biochem. Biophys. 218*, 329–334.

McManus, O. B., Musick, J. R., & Gonzalez, C. (1981) *Neurosci. Lett. 25*, 57–62.

Nishiuchi, Y., & Sakakibara, S. (1982) *FEBS Lett. 148*, 260–262.

Nishiuchi, Y., & Sakakibara, S. (1984) in *Peptides 1984* (Rangnarsson, U., Ed.) pp 537–540, de Gruyter, Berlin.

Ohkubo, T., Kobayashi, Y., Shimonishi, Y., Kyogoku, Y., Braun, W., & Gō, N. (1986) *Biopolymers 25*, s123–s134.

Olivera, B. M., McIntosh, J. M., Cruz, L. J., Luque, F. A., & Gray, W. R. (1984) *Biochemistry 23*, 2087–2090.

Olivera, B. M., Gray, W. R., Zeikus, R., McIntosh, J. M., Varga, J., Rivier, J., de Santos, V., & Cruz, L. J. (1985) *Science 230*, 1338–1343.

Olivera, B. M., Cruz, L. J., de Santos, V., LeCheminant, G. W., Griffin, D., Zeikus, R., McIntosh, J. M., Galyean, R., Varga, J., Gray, W. R., & Rivier, J. (1987) *Biochemistry 26*, 2086–2090.

Pauling, P., & Petcher, T. J. (1973) *Chem. Biol. Interact. 6*, 351–365.

Rance, M., Sorenson, O. W., Bodenhausen, G., Wagner, G., Ernst, R. R., & Wüthrich, K. (1983) *Biochem. Biophys. Res. Commun. 117*, 479–485.

Spence, I., Gillessen, D., Gregson, R. P., & Quinn, R. J. (1977) *Life Sci. 21*, 1759–1770.

States, D. J., Haberkorn, R. A., & Ruben, D. J. (1982) *J. Magn. Reson. 48*, 286–292.

Torchia, D. A. (1972) *Biochemistry 11*, 1462–1468.

Tsernoglou, D., & Petsko, G. A. (1976) *FEBS Lett. 68*, 1–4.

Wemmer, K., & Kallenbach, N. R. (1983) *Biochemistry 22*, 1901–1906.

Williamson, M. P., Havel, T. F., & Wüthrich, K. (1985) *J. Mol. Biol. 182*, 295–315.

Wüthrich, K. (1986) *NMR of Proteins and Nucleic Acids*, Wiley, New York.

Wüthrich, K., Billeter, M., & Braun, W. (1984) *J. Mol. Biol. 180*, 715–740.

Yang, C. C. (1974) *Toxicon 12*, 1–43.